Journal of Computational and Applied Mathematics 259 (2014) 752–759

Contents lists available at ScienceDirect

Journal of Computational and Applied Mathematics

journal homepage: www.elsevier.com/locate/cam

A multidimensional characteristic-based method for making incompressible flow calculations on unstructured grids

M.Y. Hashemi [a,*], K. Zamzamian [b]

[a] Department of Mechanical Engineering, Azarbaijan Shahid Madani University, Tabriz, Iran
[b] Department of Mechanical Engineering, Tabriz branch, Islamic Azad University, Tabriz, Iran

ARTICLE INFO

Article history:
Received 11 February 2013
Received in revised form 1 May 2013

Keywords:
Artificial compressibility
Multidimensional characteristic
Unstructured grid
Navier–Stokes equations

ABSTRACT

This paper presents a new multidimensional characteristic-based scheme (*MCB*) for numerical simulation of incompressible flows on unstructured grids in conjunction with the artificial compressibility method. The original *MCB* scheme has been proposed by the authors already and this research is the extension of the aforementioned scheme to unstructured grids. The significant difference between *MCB* and the conventional characteristic-based scheme (*CB*) is the multidimensional nature of the scheme, which allows information to propagate in any direction instead of only normal to the cell interface. In addition, local time stepping and the residual smoothing technique have been used for convergence acceleration. The accuracy and utility of the proposed scheme have been studied by means of numerical tests for different Reynolds numbers and the results obtained using the new scheme are in good agreement with the standard benchmark solution in the literature.

1. Introduction

The main problem of computational fluid dynamics (CFD) for configurations with complex geometry is mesh generation. The structured grid methods have a disadvantage for complex geometries [1]. The main advantage of the unstructured grid methods is the facility of grid generation for complex configurations [2]. However, the computational costs and memory requirements are generally higher than for their structured grid counterparts.

The original characteristic-based method (*CB*) for the artificial compressibility approach [3] for solving the incompressible flow equations was proposed by Drikakis et al. [4]. Then the revised *CB* method was used on unstructured grids for incompressible flow solutions by X. Su et al. [5]. The multidimensional upwind characteristic-based (*MCB*) method was proposed by Zamzamian and Razavi [6] for solving the incompressible flow equations on a structured grid; it is based on the artificial compressibility method. They showed that the *MCB* scheme is robust and powerful for modeling incompressible viscous flows and for achieving high accuracy and remarkable advantages in convergence rate with respect to the conventional *CB* scheme. The main objective of the present paper is to use the efficient *MCB* method on an unstructured grid.

2. The governing equations

The Navier–Stokes equations for two-dimensional incompressible flows modified by artificial compressibility can be expressed as

$$\oint_{\Omega} \frac{\partial \mathbf{W}}{\partial t} dV + \oint_{C} (\mathbf{F}^I dS_x + \mathbf{G}^I dS_y) = \frac{1}{Re} \oint_{C} (\mathbf{F}^V dS_x + \mathbf{G}^V dS_y) \tag{1}$$

* Corresponding author. Tel.: +98 9127044971.
E-mail address: m.y.hashemi@azaruniv.ac.ir (M.Y. Hashemi).

0377-0427/$ – see front matter © 2013 Elsevier B.V. All rights reserved.
http://dx.doi.org/10.1016/j.cam.2013.06.008

where

$$\mathbf{W} = \begin{bmatrix} p \\ u \\ v \end{bmatrix}, \qquad \mathbf{F}^I = \begin{bmatrix} \beta u \\ u^2 + p \\ uv \end{bmatrix}, \qquad \mathbf{G}^I = \begin{bmatrix} \beta v \\ vu \\ v^2 + p \end{bmatrix},$$
$$\mathbf{F}^V = \begin{bmatrix} 0 \\ \dfrac{\partial u}{\partial x} \\ \dfrac{\partial v}{\partial x} \end{bmatrix}, \qquad \mathbf{G}^V = \begin{bmatrix} 0 \\ \dfrac{\partial v}{\partial x} \\ \dfrac{\partial v}{\partial y} \end{bmatrix}. \tag{2}$$

Here $\mathbf{W}$ is the vector of primitive variables, and $\mathbf{F}^I$, $\mathbf{G}^I$ and $\mathbf{F}^V$, $\mathbf{G}^V$ are convective and viscous flux vectors, respectively. The artificial compressibility parameter and Reynolds number are shown as β and Re, respectively. The above equations have been nondimensionalized on the basis of the following scalings:

$$x = \frac{x^*}{l^*}, \qquad y = \frac{y^*}{l^*}, \qquad t = \frac{t^*}{l^*/U_{ref}},$$
$$u = \frac{u^*}{U_{ref}}, \qquad v = \frac{v^*}{U_{ref}}, \qquad p = \frac{p^* - p_{ref}}{\rho_{ref} U_{ref}^2}. \tag{3}$$

The discretized form of Eqs. (1) at cell i is obtained:

$$A_i \frac{\partial \mathbf{W}_i}{\partial t} + \sum_{j=1}^{m} \mathbf{F}_j^I (\Delta S_x)_j + \sum_{j=1}^{m} \mathbf{G}_j^I (\Delta S_y)_j = \frac{1}{Re} \left[\sum_{j=1}^{m} \mathbf{F}_j^V (\Delta S_x)_j + \sum_{j=1}^{m} \mathbf{G}_j^V (\Delta S_y)_j \right] \tag{4}$$

where A_i is the cell area and m is the number of edges for any cells. Examples of computational unstructured grids that are used for finite-volume *MCB* flow solvers are shown in Fig. 3.

3. The solution algorithm

3.1. The two-dimensional characteristic structure for artificial compressibility equations

To derive the characteristic relations of incompressible flows, their corresponding "Euler equations" are considered [7]. These equations modified by artificial compressibility for deriving two-dimensional characteristic structures are

$$\frac{\partial p}{\partial t} + \beta \frac{\partial u}{\partial x} + \beta \frac{\partial v}{\partial y} = 0$$
$$\frac{\partial u}{\partial t} + u \frac{\partial u}{\partial x} + u \frac{\partial u}{\partial y} + \frac{\partial p}{\partial x} = 0 \tag{5}$$
$$\frac{\partial v}{\partial t} + u \frac{\partial v}{\partial x} + u \frac{\partial v}{\partial y} + \frac{\partial p}{\partial y} = 0.$$

To obtain the characteristic structure of equations, a characteristic surface in the form of $f(x, y, t) = 0$ is assumed. Using the kinematics relations for relating the partial derivatives to exact derivatives corresponding to the assumed surface, one gets the following system of equations [8,9]:

$$\begin{bmatrix} \dfrac{f_t}{\beta} & f_x & f_y \\ f_x & \psi & 0 \\ f_y & 0 & \psi \end{bmatrix} \begin{bmatrix} dp \\ du \\ dv \end{bmatrix} = \begin{bmatrix} 0 \\ 0 \\ 0 \end{bmatrix} \tag{6}$$

where the subscripts stand for the partial differentiation and ψ is defined as

$$\psi = \frac{\partial f}{\partial t} + u \frac{\partial f}{\partial x} + v \frac{\partial f}{\partial y}. \tag{7}$$

For compatibility requirements of Eqs. (6), the determinant of the coefficient matrix is set to zero; hence,

$$\psi = 0, \qquad \psi = \frac{\beta}{f_t} \left(f_x^2 + f_y^2 \right). \tag{8}$$

We assumed the pseudo-velocity vector $\mathbf{V} = (u, v, 1)$ and the normal vector to the characteristic surface $\mathbf{n} = (\cos(\varphi), \sin(\varphi), n_t)$ like for the compressible Euler equations [10], in which φ shows the wave direction. Expressing Eq. (8) in terms of vectors $\mathbf{V}$ and $\mathbf{n}$, two types of characteristic surface corresponding to the following relations are obtained:

$$\mathbf{V} \bullet \mathbf{n} = 0, \qquad \mathbf{V} \bullet \mathbf{n} = \frac{\beta}{n_t} \tag{9}$$

where $n_t = f_t/\sqrt{f_x^2 + f_x^2}$ denotes the t-component of the normal vector. By some mathematical operations, n_t takes the following forms:

$$n_t = \frac{-(u\cos(\varphi) + v\sin(\varphi)) \pm \sqrt{(u\cos(\varphi) + v\sin(\varphi))^2 + 4\beta}}{2} = n_1, n_2. \tag{10}$$

Regarding the dual roots of the second relation in Eqs. (9) as a function of n_t, like for the compressible Euler equations, dual characteristic surfaces would exist. With straightforward mathematical operations it can be proven that the roots always have different signs. This depicts the growth of zones of influence and dependence around the pseudo-streamlines. It can be shown that the characteristic path equations are given by

$$\frac{dx}{dt} = u - \frac{\beta}{n_t}\cos(\varphi), \qquad \frac{dy}{dt} = v - \frac{\beta}{n_t}\sin(\varphi) \tag{11}$$

where φ is the wave angle. As is seen in Fig. 1, for any angle in the range $0 \le \varphi \le 2\pi$ there exist two bicharacteristics. The compatibility relations corresponding to characteristic paths (Eq. (9)) are obtained as

$$\frac{\beta}{n_t}du + \cos(\varphi)dp = 0, \qquad \frac{\beta}{n_t}dv + \sin(\varphi)dp = 0. \tag{12}$$

Eqs. (12) are valid for both $n_t = n_1, n_2$, showing the governing compatibility relations along bicharacteristics. For more details see [6,11].

3.2. The numerical scheme for the evaluation of convective fluxes on unstructured grids

Using the compatibility equations (12), a new multidimensional characteristic-based upwind scheme has been presented here. As seen in Fig. 2, four characteristic paths corresponding to four wave angles $\varphi_1, \varphi_2, \varphi_3, \varphi_4$ have been selected and the compatibility equations (12) along them are used for evaluating convective fluxes between two cells "R" and "L". When angle "φ_1" (Fig. 2) is smaller than $\pi/4$, discretization is done by using the first relation of Eqs. (12) for "φ_3, φ_4" and the second one for "φ_1, φ_2", and when "φ_1" is bigger than $\pi/4$ vice versa. For example, in the case of $\varphi_1 < \pi/4$, the discretized equations are in the following form:

$$\begin{aligned} &p^* - p_1 + A(u^* - u_1) = 0, \qquad p^* - p_2 + B(u^* - u_2) = 0,\\ &p^* - p_3 + C(v^* - v_3) = 0, \qquad p^* - p_4 + D(v^* - v_4) = 0 \end{aligned} \tag{13}$$

where p^*, u^* and v^* are the values at the cell interface and A, B, C, D can be obtained from Eqs. (10)–(12) as follows:

$$\begin{aligned} &\Omega_1 = u_1\cos(\varphi_1) + v_1\sin(\varphi_1), \qquad \Omega_2 = u_2\cos(\varphi_2) + v_2\sin(\varphi_2)\\ &A = \frac{2\beta}{\cos(\varphi_1)\left[-\Omega_1 + \sqrt{\Omega_1^2 + 4\beta}\right]}, \qquad B = \frac{2\beta}{\sin(\varphi_1)\left[-\Omega_1 + \sqrt{\Omega_1^2 + 4\beta}\right]},\\ &C = \frac{2\beta}{\cos(\varphi_2)\left[-\Omega_2 + \sqrt{\Omega_2^2 + 4\beta}\right]}, \qquad D = \frac{2\beta}{\sin(\varphi_2)\left[-\Omega_2 + \sqrt{\Omega_2^2 + 4\beta}\right]}. \end{aligned} \tag{14}$$

p^*, u^* and v^* are calculated with Eq. (13) using flow properties at points 1, 2, 3 and 4 in the previous time level. Then they are used to determine convective fluxes at the cell interface. The value of u^* is determined from the first and second equations of Eq. (13) and v^* is determined from the third and fourth ones. The final value of p^* is assumed to be the arithmetic average of values obtained from two sets of equations (first–second and third–fourth in Eq. (13)). Flow properties at points 1, 2 are set to neighborhood cell values and for points 3, 4, interpolated from two cells containing the assumed face (cells "L, R" in Fig. 2). By using the flow values at points 3 and 4 in order to evaluate the interface values at face j, we take into account the real two-dimensional nature of the flow and do not assume any one-dimensional assumptions.

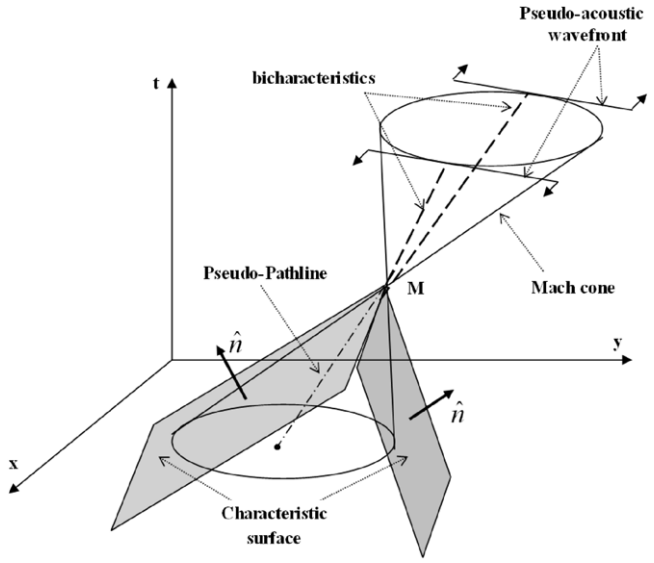

Fig. 1. Characteristic structure for incompressible flow defined by artificial compressibility equations.

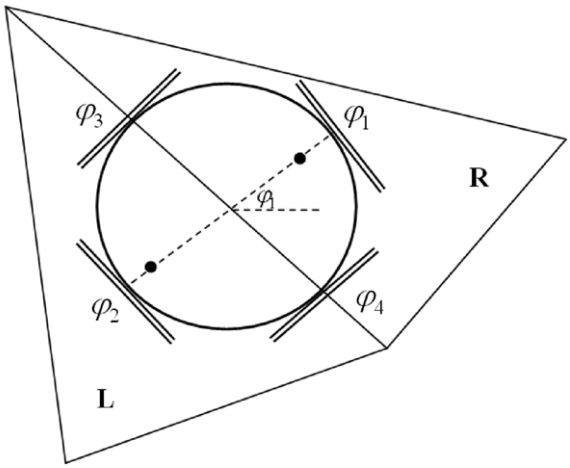

Fig. 2. *MCB* stencil for evaluating convective fluxes.

4. Time discretization

An explicit fourth-order Runge–Kutta scheme with modified coefficients [12] is used for time discretization of spatially discretized equations as follows:

$$\begin{aligned}
&\frac{\partial \mathbf{W}_i}{\partial t} + \mathbf{R}_i(\mathbf{W}) = 0\\
&\mathbf{W}_i^{(0)} = \mathbf{W}_i^{(n)}\\
&\mathbf{W}_i^{(1)} = \mathbf{W}_i^{(0)} - \alpha_1.\Delta t \cdot \mathbf{R}_i(\mathbf{W}^{(0)})\\
&\cdots\\
&\mathbf{W}_i^{(4)} = \mathbf{W}_i^{(3)} - \alpha_4.\Delta t \cdot \mathbf{R}_i(\mathbf{W}^{(3)})\\
&\mathbf{W}^{(n+1)} = \mathbf{W}^{(4)}\\
&\alpha_1 = 0.333, \qquad \alpha_2 = 0.2667, \qquad \alpha_3 = 0.5, \qquad \alpha_4 = 1.0
\end{aligned} \tag{15}$$

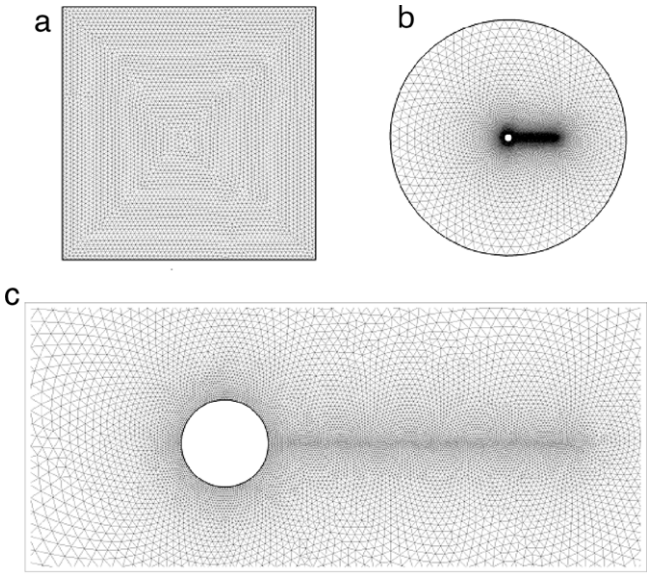

Fig. 3. Unstructured numerical grids used for a test cases (*a*: coarse grid of the cavity test case, *b*: grid over the circular cylinder and *c*: close view of the grid over the circular cylinder).

where the $\mathbf{R}_i$ are residuals that contain the convective and viscous flux as follows:

$$\mathbf{R}_i = \sum_{j=1}^{m} \mathbf{F}_j^I (\Delta S_x)_j + \sum_{j=1}^{m} \mathbf{G}_j^I (\Delta S_y)_j - \frac{1}{Re}\left[\sum_{j=1}^{m} \mathbf{F}_j^V (\Delta S_x)_j + \sum_{j=1}^{m} \mathbf{G}_j^V (\Delta S_y)_j\right]. \tag{16}$$

Local time stepping at any cells can be evaluated with a convective term as [13]

$$\Delta t_i = CFL \frac{A_i}{\sum_{j=1}^{m}\left[|u_e \Delta S_x + v_e \Delta S_y| + \sqrt{u_e^2 + v_e^2 + \beta}\sqrt{\Delta S_x^2 + \Delta S_y^2}\right]_j} \tag{17}$$

where *CFL* is the Courant number and $u_e = 0.5(u_L + u_R)$, $v_e = 0.5(v_L + v_R)$. To accelerate convergence, local time stepping is used in any explicit iterations [14]. In addition, the original residuals may be replaced by the smoothed residuals by solving the implicit equation [12]

$$\overline{\mathbf{R}}_i = \mathbf{R}_i + \epsilon \nabla^2 \overline{\mathbf{R}}_i. \tag{18}$$

At each cell i, $\nabla^2 \overline{\mathbf{R}}_i$ represents the undivided Laplacian of the most recent residuals, and is the smoothing coefficient that is chosen equal to 0.5 in this research.

5. Results

To compare the accuracy of the newly proposed *MCB* scheme on unstructured grids, lid-driven cavity flow and flow over the circular cylinder at different Reynolds numbers are reported in this paper.

5.1. Cavity flow

At first, to verify the ability of the *MCB* scheme on unstructured grids, incompressible steady flow at $Re = 100, 400, 3200$ (based on moving wall velocity and cavity length) are presented with 8088, 15 243 and 22 469 triangular cells respectively. Results obtained for the u-velocity profile along the vertical line and the v-velocity profile along the horizontal line passing through the center of the cavity using the *MCB* scheme are presented in Fig. 4. As shown, the results obtained are in good agreement with the Ghia et al. [15] benchmark solution.

A grid study is performed at $Re = 10\,000$ by using three computational unstructured triangular meshes including 8088, 22 464 and 44 082 cells, regarded as coarse, medium and fine grids, respectively. The coarse generated grid in the cavity is shown in Fig. 3. There are 60 edges on any wall. Fig. 5 presents the u-velocity profile along a vertical line and the v-velocity profile along a horizontal line passing through the cavity center. These profiles are in good agreement with the well known benchmark results of Ghia et al. [15] that are shown by symbols in the figures. Fig. 6 shows streamlines of the flow field for the different Reynolds numbers obtained using the *MCB* scheme.

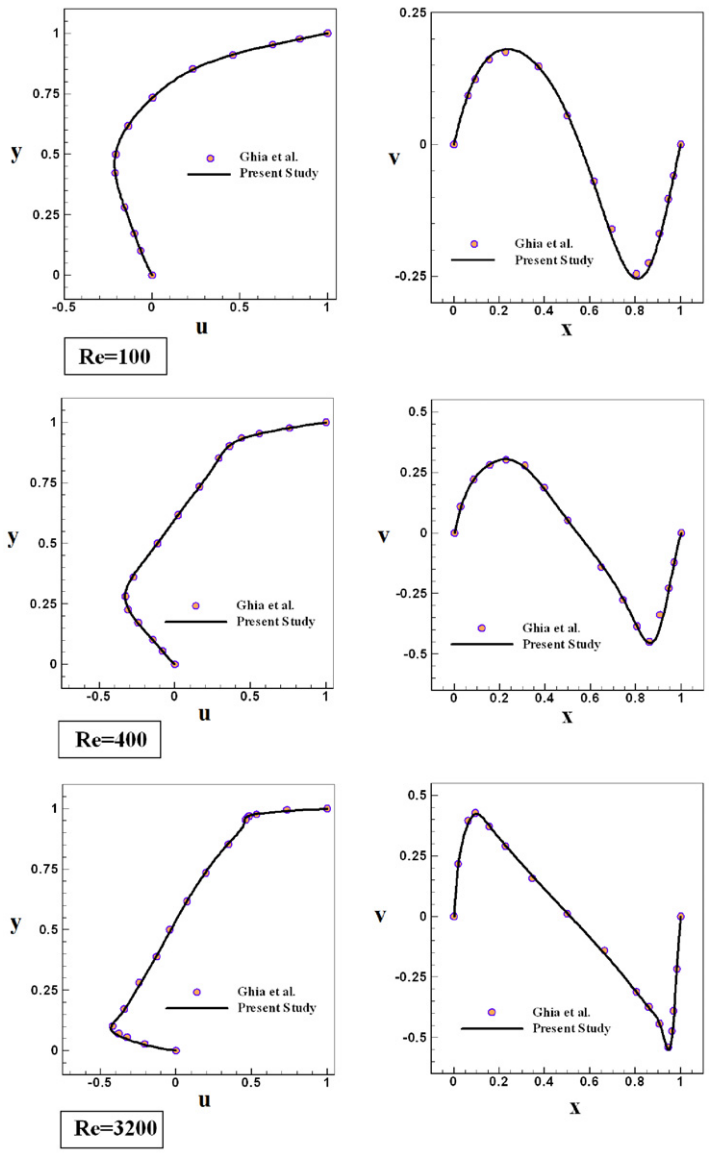

Fig. 4. Comparison of the predicted mid-plane velocity profiles for u and v at $Re = 100$, $Re = 400$ and $Re = 3200$.

5.2. A circular cylinder

A second test case is incompressible flow over the circular cylinder, to demonstrate the ability of the proposed method in simulation of the separated steady and unsteady flows. The far field boundary is located at a distance of 30 radii from the cylinder. The generated unstructured grid is shown in Fig. 3. The solid boundary includes 208 edges, and there are 82 edges on the far field boundary. The computational domain includes 23 380 triangular cells. The streamlines over the cylinder are shown in Fig. 7 for five Reynolds numbers. The computed drag coefficients are compared with the reliable numerical data in Table 1. The results are in good agreement with other reported numerical solutions.

6. Conclusions

A new multidimensional characteristic-based scheme *MCB* was presented for numerical simulation of incompressible flows on unstructured grids. The proposed *MCB* scheme is used to solve problems of steady incompressibility-driven cavity flow and flow over circular cylinders at different Reynolds numbers. The capabilities of the method were demonstrated by comparing the results with the available benchmark solutions from the literature and the results are in good agreement with them.

Table 1
Computed drag coefficients at different Reynolds numbers.

$Re = (\rho VD)/\mu$	Drag coefficient (C_D)		
	Present results	Zamzamian and Razavi [6]	Ding et al. [16]
10	2.91	2.98	3.07
20	2.14	2.03	2.18
40	1.62	1.55	1.713
100	1.34	1.33	
200	1.31	1.32	

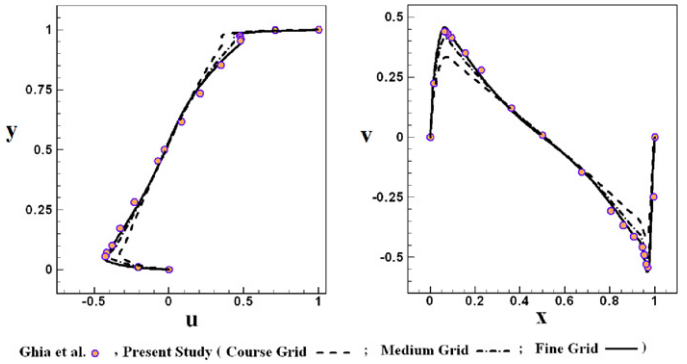

Fig. 5. Comparison of the predicted mid-plane velocity profiles for u and v at $Re = 10{,}000$.

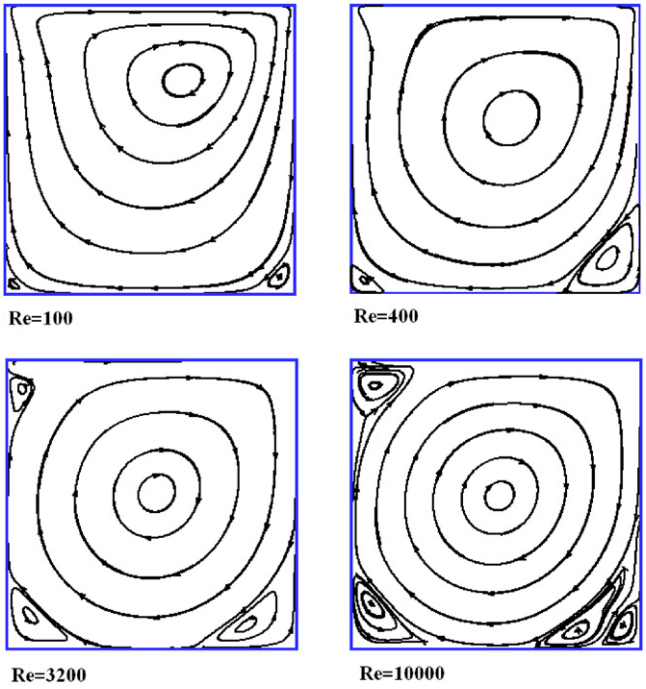

Fig. 6. Streamlines of the flow field for the different Reynolds numbers.

7. Figures and drawings

See Figs. 1–7.

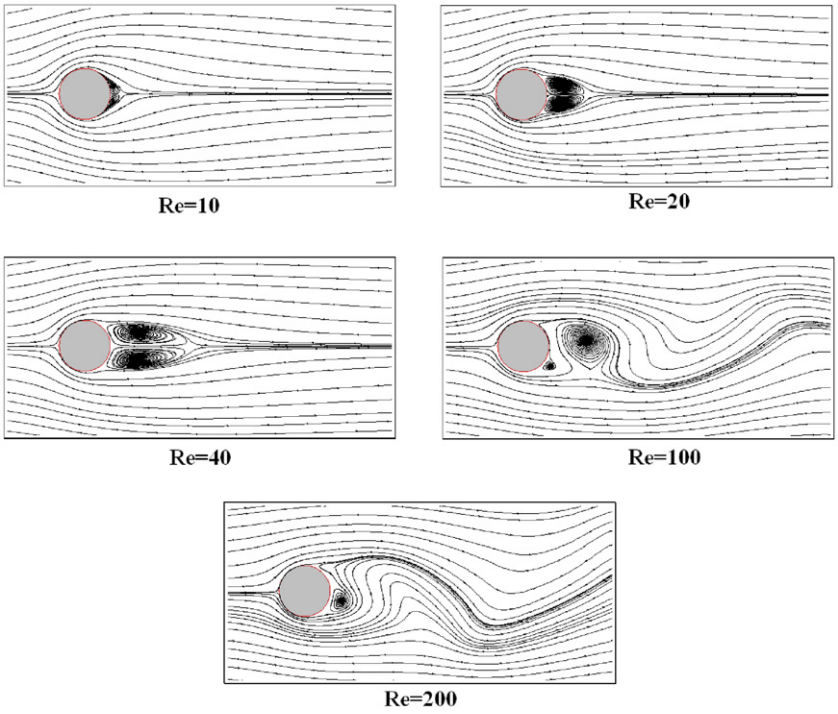

Fig. 7. Streamlines around the circular cylinder for the different Reynolds numbers.

References

[1] J.F. Thompson, F.C. Thomas, C.W. Mastin, Automated numerical generation of body fitted curvilinear co-ordinate system for field containing any number of arbitrary 2D bodies, J. Comput. Phys. 15 (1974) 299–319.
[2] O. Hassan, E.J. Probert, K. Morgan, Unstructured mesh procedures for the simulation of three-dimensional transient compressible inviscid flows with moving boundary components, Internat. J. Numer. Methods Fluids 27 (1998) 41–55.
[3] A.J. Chorin, A numerical method for solving incompressible viscous flow problems, J. Comput. Phys. 2 (1967) 12–26; J. Comput. Phys. 135 (1997) 118–125.
[4] D. Drikakis, P.A. Govatsos, D.E. Papatonis, A characteristic based method for incompressible flows, Internat. J. Numer. Methods Fluids 19 (1994) 667–685.
[5] X. Su, Y. Zhao, X. Huang, On the characteristics-based ACM for incompressible flows, J. Comput. Phys. 227 (2007) 1–11.
[6] Kamiar Zamzamian, Seyed Esmail Razavi, Multidimensional upwinding for incompressible flows based on characteristics, J. Comput. Phys. 227 (2008) 8699–8713.
[7] Y. Zhao, B. Zhang, A high-order characteristics upwind FV method for incompressible flow and heat transfer simulation on unstructured grids, Comput. Methods Appl. Mech. Eng. 190 (2000) 733–756.
[8] S.E. Razavi, Far field boundary conditions for computation of compressible aerodynamic flows, Ph.D. Thesis, Department of Mechanical Engineering, McGill university, Montreal, Canada, 1995.
[9] L. Fox, Numerical Solution of Ordinary and Partial Differential Equations, Pergamon Press, Oxford, 1962.
[10] Hoffman Zacrow J.D., Gas Dynamics, Vol. 2, John Wiley and Sons, New York, 1976.
[11] S.E. Razavi, K. Zamzamian, A. Farzadi, Genuinely multidimensional characteristic-based scheme for incompressible flows, Internat. J. Numer. Methods Fluids 57 (2008) 929–949.
[12] Y. Hashemi, A. Jahangirian, Implicit fully mesh-less method for compressible viscous flow calculations, J. Comput. Appl. Math. 235 (2011) 4677–4700.
[13] G. May, A. Jameson, Unstructured algorithms for inviscid and viscous flows embedded in a unified solver architecture Flo3xx, in: AIAA 43rd Aerospace Sciences Meeting, No. 0318, Reno, Nevada, January, 2005.
[14] M.Y. Hashemi, A. Jahangirian, An efficient implicit mesh-less method for compressible flow calculations, Internat. J. Numer. Methods Fluids 30 (2011) 754–770.
[15] U. Ghia, K.N. Ghia, C.T. Shin, High-Re solutions for incompressible flow using the Navier–Stokes equations and a multigrid method, J. Comput. Phys. 48 (1982) 387–411.
[16] H. Ding, C. Shu, K.S. Yeo, D. Xu, Simulation of incompressible viscous flow past a circular cylinder by hybrid FD scheme and meshless least-square based finite difference method, Comput. Methods Appl. Mech. Eng. 193 (2004) 727–744.